6

Research Article

Piotr Czubak and Marek Gajowy*

Influence of selected physical parameters on vibroinsulation of base-exited vibratory conveyors

https://doi.org/10.1515/eng-2022-0033 received May 17, 2021; accepted December 13, 2021

Abstract: Vibrating conveyors tend to transfer dynamic forces to the ground. One way to vibroinsulate such systems from the environment is to use dynamic methods to eliminate vibrations. Due to this phenomenon, the forces transferred to the ground are reduced. This article attempts to identify important elements determining the design of an antiresonance-type conveyor. The study of dynamic phenomena was based on two models of such conveyors with two and six degrees of freedom (with the phenomenon of self-synchronization). In this work, the impacts of various types of suspension and the ratio of the body mass to the mass of the conveyor trough on forces transmitted to the ground are analysed.

Keywords: dynamic damper, self-synchronization, vibroinsulation, vibrating conveyor

1 Introduction

Among devices for transporting loose materials of a distributed mass, vibratory conveyors are essential. They are used for transporting at short distances, not exceeding several dozens of meters. This type of conveyor was patented for the first time in 1891 by Fischer [1]. Conveyors operating on the base of the dynamic elimination of vibrations (in a similar manner to Frahm's eliminator [2]), in which the vibroinsulating frame is excited for vibrations and the trough constitutes the eliminator, are

[3]. These authors analysed the conveyor behaviour around the assumed excitation frequency (being, according to their work, the vibroinsulating Frahm's damper). They noticed that in this type of conveyor, due to the fastening of the forcing system to the mass, which in theory is not vibrating, their service life and the conveyor suspension service life were increasing. Investigations into this type of structure called "antiresonance" were also performed by Liu and Sun [4], Liu et al. [5]. One of the first, this type of construction, called the base-excited or resonance conveyor, was investigated by Long and Tsuchiya [6] and Carmichael [7]. Liu et al. [8] investigated the possibility of controlling the excitation frequency around the work point, while Zhao and Gao [9] tested the conveyor with a frequency controlled by a proportional integral differential (PID) controller, depending on the vibration amplitude of the vibroinsulating frame. Similar investigations were performed by Ribic [10], where the forced frequency of the feeder was controlled, and by the team of Despotovic and Stojiljkovic [11], who also performed tests concerning the control of the excitation frequency of the conveyor. Among works concerning this type of conveyors are the papers of Czubak [12] – in this research, the influence of the feed material mass on forces transmitted to the foundations was analysed. Klemiato and Czubak [13] and Czubak [14] investigated the possibility of controlling the excitation frequency, allowing the reduction of forces transmitted by the loaded conveyor. One of the most recent papers of Michalczyk and Gajowy [15] is a study in which the authors investigated the basic dynamic properties of conveyor models operating on the basis of dynamic elimination. In the same work, the authors also examined, by analytical and simulation methods, amplitudes in the transient resonance of this type of dynamic systems (during the coast). Another study

was performed by Hou et al. [16], who investigated synchro-

nization stability of Frahm's system forced by two counter

a relatively new kind of conveyors. These conveyors and

feeders have wide applications in the industry in transporting feed materials of small masses. Among papers

dealing with these problems is the paper of Jiao et al.

Piotr Czubak: Department of Mechanics and Vibroacoustics, Faculty of Mechanical Engineering and Robotics, AGH University of Science and Technology, Kraków, Poland, e-mail: czubak@agh.edu.pl

^{*} Corresponding author: Marek Gajowy, Department of Mechanics and Vibroacoustics, Faculty of Mechanical Engineering and Robotics, AGH University of Science and Technology, Kraków, Poland, e-mail: mgajowy@agh.edu.pl

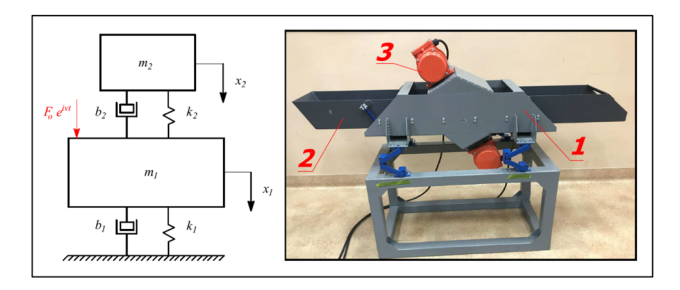


Figure 1: The scheme of operations of the antiresonance conveyor – dynamic eliminator. On the right side presented is the picture of the real antiresonance conveyor: (1) the body, (2) the gutter, and (3) one of two electrovibrators.

running vibrators. The problem of a weak antiresonance performance and poor working stability in current antiresonance vibrating machines, under the material mass fluctuation condition, was discussed by Li and Shen [17]. Among the recent papers concerning dual-mass conveyors, the publications of Sturm [18] and Strum and Pešík [19] should be noted. In these papers, the influence of dual-mass conveyors on foundations was investigated.

1.1 Discrete model of the vibratory antiresonance conveyor of two degrees of freedom (DOFs)

The scheme of the operations of the antiresonance conveyor, whose operations are based on the effect of the dynamic elimination of vibrations, is presented in Figure 1.

Frahm invented the dynamic eliminator of vibrations, intended for damping vibrations of the harmonic oscillator excited by sinusoidal – time-variable – force, in 1909 (Figure 1). When to the main mass m_1 , supported by the suspension of elasticity k_1 and damping b_1 and excited for vibrations along coordinate x_1 by force F_o e^{ivt} , the additional mass m_2 will be connected, via the suspension system of parameters k_2 and k_2 are selected in such a way that the partial frequency being at the same time the antiresonance frequency

$$\omega_{\alpha} = \sqrt{k_2/m_2}, \qquad (1)$$

is equal to the excitation frequency v, vibrations of mass m_2 stabilize in such a way as that the force in spring k_2 counterbalances – in the case when there is no damping – the excitation force $F_o e^{ivt}$ eliminating vibrations of the main mass. This effect occurs regardless of the frequency of natural vibrations of the basic system before the eliminator connection. The Frahm's eliminator system in the antiresonance

valley is surrounded from both sides by resonance zones. This valley width depends on the ratio of the eliminator mass to the main mass and in the classic case, when $m_1 >> m_2$, is relatively narrow. This is highly essential when the excitation frequency v is not constant, as it happens in the case of a soft mechanical characteristic of the drive motor.

Dynamic equations describing the above model are as follows:

$$m_1\ddot{x}_1 + k_1x_1 + k_2(x_1 - x_2) + b_1\dot{x}_1 + b_2(\dot{x}_1 - \dot{x}_2) = F_0e^{i\nu t}, m_2\ddot{x}_2 - k_2(x_1 - x_2) - b_2(\dot{x}_1 - \dot{x}_2) = 0.$$
(2)

The amplitude of the excitation force $F_o e^{ivt}$ can be described as the centrifugal force

$$F_0 = mrv^2. (3)$$

The excitation force is a character of translational and harmonic force. Predicting the solution by Thomson [20] in a form:

$$x_1 = Ae^{i\nu t}$$

$$x_2 = Be^{i\nu t}$$
(4)

provides the solution – in the form of absolute values of *A* and *B* amplitudes obtained in the form:

$$|A| = \frac{\sqrt{(mm_2rv^4 - k_2mrv^2)^2 + (b_2mrv^3)^2}}{\sqrt{(k_1m_2v^2 - k_1k_2 + k_2m_1v^2 + k_2m_2v^2 - m_1m_2v^4 + b_1b_2v^2)^2}},$$

$$|B| = \frac{\sqrt{(k_2mrv^2)^2 + (b_2mrv^3)^2}}{\sqrt{(k_2mrv^2)^2 + (b_2mrv^3)^2}}.$$

$$|B| = \frac{\sqrt{(k_2mrv^2)^2 + (b_2mrv^3)^2}}{\sqrt{(k_1m_2v^2 - k_1k_2 + k_2m_1v^2 + k_2m_2v^2 - m_1m_2v^4 + b_1b_2v^2)^2}}.$$

$$|B| = \frac{\sqrt{(k_2mrv^2)^2 + (b_2mrv^3)^2}}{\sqrt{(k_1m_2v^2 - k_1k_2 + k_2m_1v^2 + k_2m_2v^2 - m_1m_2v^4 + b_1b_2v^2)^2}}.$$

$$|B| = \frac{\sqrt{(mm_2rv^4 - k_2mrv^2)^2 + (b_2mrv^3)^2}}{\sqrt{(k_2mrv^2)^2 + (b_2mrv^3)^2}}.$$

$$|B| = \frac{\sqrt{(mm_2rv^4 - k_2mrv^2)^2 + (b_2mrv^3)^2}}{\sqrt{(k_2mrv^2)^2 + (b_2mrv^3)^2}}.$$

$$|B| = \frac{\sqrt{(mm_2rv^4 - k_2mrv^2)^2 + (b_2mrv^3)^2}}{\sqrt{(k_2mrv^2)^2 + (b_2mrv^3)^2}}.$$

$$|B| = \frac{\sqrt{(mm_2rv^4 - k_2mrv^2)^2 + (b_2mrv^3)^2}}{\sqrt{(k_2mrv^2)^2 + (b_2mrv^3)^2}}.$$

$$|B| = \frac{\sqrt{(mm_2rv^4 - k_2mrv^2)^2 + (b_2mrv^3)^2}}{\sqrt{(k_2mrv^2)^2 + (b_2mrv^3)^2}}.$$

$$|B| = \frac{\sqrt{(mm_2rv^4 - k_2mrv^2)^2 + (b_2mrv^3)^2}}{\sqrt{(k_2mrv^2)^2 + (b_2mrv^3)^2}}.$$

$$|B| = \frac{\sqrt{(mm_2rv^4 - k_2mrv^2)^2 + (b_2mrv^3)^2}}{\sqrt{(k_2mrv^2)^2 + (b_2mrv^3)^2}}.$$

$$|B| = \frac{\sqrt{(mm_2rv^4 - k_2mrv^2)^2 + (b_2mrv^3)^2}}{\sqrt{(k_2mrv^2)^2 + (b_2mrv^3)^2}}.$$

$$|B| = \frac{\sqrt{(mm_2rv^4 - k_2mrv^2)^2 + (b_2mrv^3)^2}}{\sqrt{(k_2mrv^2)^2 + (b_2mrv^3)^2}}.$$

1.2 Parameter selection

The following parameters of the system where taken from the required mass ratio (m_1 to m_2). The trough mass was assumed at the level $m_2 = 20$ kg, which corresponds to the real mass of the trough of the conveyor shown in Figure 1. At the beginning, in order to obtain the large width of the antiresonance valley considered by Den Hartog [21], the body mass m_1 was selected to be of the same value as the mass of the trough. The body of the machine shown in Figure 1 was constructed in such a way that its weight was approximately 30 kg (redimensioning for safety reasons). The work hereby proves that, from the point of view of the discrete model, the best solution is when the ratio of the body weight to the trough weight is 1:1. However, operations of lightening down the body structure, utilizing advanced designing methods, are necessary. Due to this, the following data are assumed:

$$m_1 = 20 \text{ kg}, \quad m_2 = 20 \text{ kg}.$$

Parameter values for determining the excitation force (3) are assumed in such a way to obtain the coefficient of throw equal to approximately 3.8 [22]:

$$m = 2.98 \text{ kg},$$

 $r = 0.02 \text{ m}.$

v = 157 rad/s.

Stiffness and damping of suspensions:

For assuring the same static deflection for various masses m_1 , the coefficient of elasticity k_1 is defined in equation (6). Value 66,800 N/m comes from the vibroinsulation condition considered by Michalczyk and Cieplok [23] for the sum of masses $m_1 = 20$ kg and $m_2 = 20$ kg:

$$k_1(m_1) = 66,800 \cdot \frac{m_1 + m_2}{20 + m_2} = 66,800$$

 $\cdot \frac{m_1 + 20}{20 + 20} [\text{N/m}].$ (6)

According to (1)

$$k_2 = v^2 \cdot m_2 = 492,980 \text{ N/m}.$$

The equivalent viscous damping coefficient is represented by expressions:

$$b_{1} = \frac{\psi_{1}k_{1}}{2\pi\nu},$$

$$b_{2} = \frac{\psi_{2}k_{2}}{2\pi\nu},$$
(7)

where $\psi_1 = 0.4$ – energy absorption coefficient for rubber elements described by Michalczyk [22] and $\psi_2 = 0.04$ – energy absorption coefficient for elements of flat metal spring type described by Michalczyk [22].

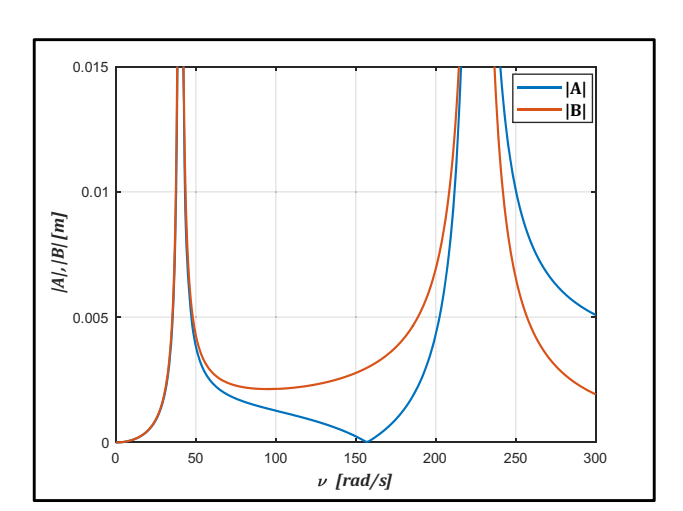


Figure 2: Amplitude–frequency characteristics of vibrations of masses m_1 and m_2 .

1.3 Results

For the assumed data, the diagrams of the amplitude displacements $A(\nu)$ and $B(\nu)$ at the quasi-stationary value of the excitation frequency from the range $\nu = 0-300$ rad/s are presented in Figure 2.

In the steady state, at the antiresonance frequency of 157 rad/s, the minimization of vibrations of mass m_1 occurs (Figure 2). As it results from Figure 3, the vibration amplitude of both masses is not changing – in the steady state – with the smaller mass increasing.

1.4 Force transmitted to the foundation and the influence of the energy absorption coefficient of the supporting elements on the vibroinsulation

The force transmitted to the foundation is generated by the suspension of elasticity k_1 and the equivalent damping factor b_1 , and its formula (8) is as follows:

$$R = k_1 \cdot |A| + b_1 \cdot |A| \cdot \nu \cdot i. \tag{8}$$

The dependence of the force transmitted to the foundation, in the steady state at the antiresonance (working) frequency, on the body mass m_1 and constant mass m_2 was derived. It should be mentioned that along with changes in the mass value m_1 , the elasticity of support k_1 was changing – in accordance with formula (6) – in order to maintain the same static deflection of the mass m_1 .

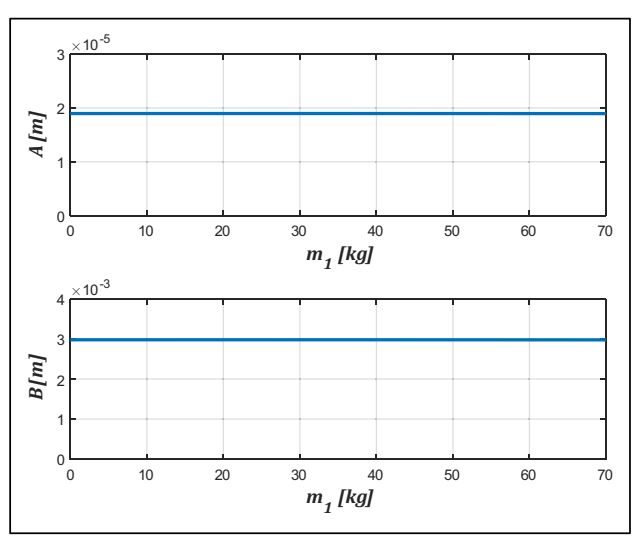


Figure 3: Vibration amplitude of masses m_1 and m_2 in the steady state as a mass m_1 functions with angular speed v = 157 rad/s.

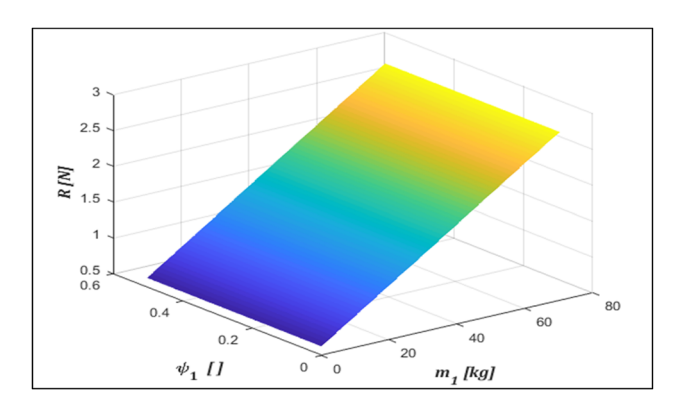


Figure 4: The simultaneous influence of mass m_1 and the energy absorption coefficient of the suspension ψ_1 on the force transmitted to the foundation at parameters from Section 1.2 for steady excitation frequency v=157 rad/s.

Figure 4 shows that the application of a lower mass m_1 leads to the limitation of the force transmitted to the foundation in the work point. The smaller force transmitted to the foundation results partially from the lower support stiffness but mainly from the fact that the anti-resonance vibroinsulation is more efficient when the mass of the eliminator (trough) is higher than the excited mass. It is also seen from Figure 4 that the energy absorption coefficient of the support ψ_1 of mass m_1 does not influence forces transmitted to the foundation at the steady state for $\nu = 157 \, \text{rad/s}$.

The dynamic influence on the foundation is not increasing with the damping increase of this part of the suspension system. This is related to the fact that the excited mass in the steady state has a very small vibration amplitude, which means that the damping of the frame suspension system does not have a high influence on the system.

The influence of the energy absorption coefficient of suspension ψ_2 of eliminator mass m_2 on mass m_1 is different (Figure 5). The smaller the damping coefficient, the more efficient the antiresonance vibroinsulation. The force transmitted to the foundation decreases in direct proportion to the decrease of the value of the equivalent damping factor b_2 , which suggests the application of the steel leaf suspension of a low damping factor.

The force transmitted to the foundation in the resonance zone at frequency $v \approx 40 \, \text{rad/s}$ (for the quasi-stationary state) changes to a small degree only with mass m_1 change, whereas when mass m_1 decreases, the width of the antiresonance zone increases, which improves the operation stability (Figure 6). At frequency $v = 157 \, \text{rad/s}$, forces transmitted to the foundation decrease when mass m_1 decreases (Figure 6).

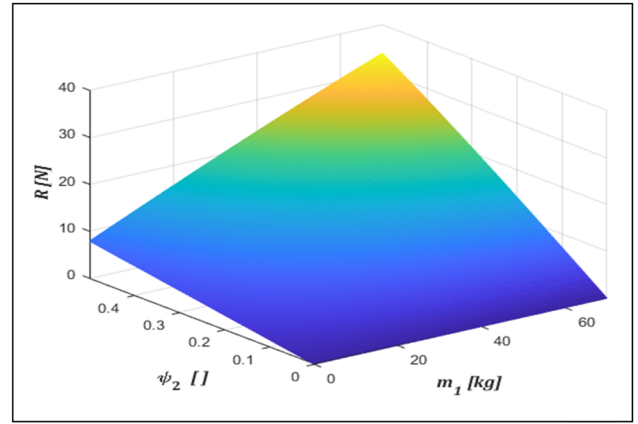


Figure 5: The simultaneous influence of mass m_1 and the energy absorption coefficient of the suspension ψ_2 on the force transmitted to the foundation at parameters from Section 1.2 for steady excitation frequency v = 157 rad/s.

The influence of ψ_1 on forces transmitted to the foundations in the resonance zone $v \approx 40$ rad/s for constant masses $m_1 = 20$ kg and $m_2 = 20$ kg is essential. The higher the coefficient ψ_1 , the lower the value of the force transmitted to the foundation (Figure 7). However in the steady state of antiresonance zone, this influence is negligible (Figure 4). This suggests the application of the rubber-type suspension with strong damping characteristics, e.g. Rosta type described by Cieplok et al. [24].

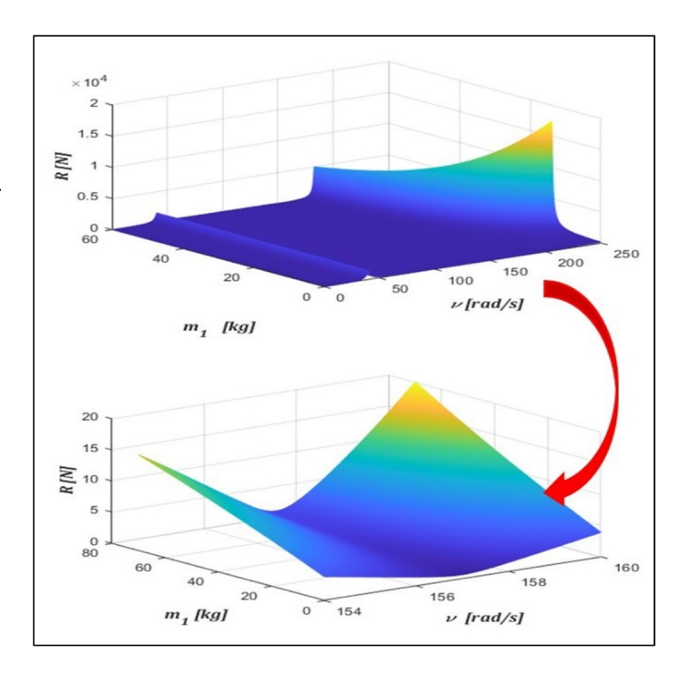


Figure 6: The absolute value of reaction force $R(v, m_1)$ at parameters from Section 1.2.

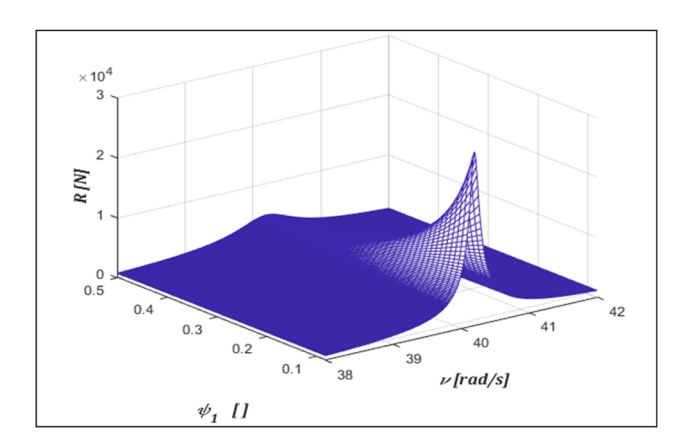


Figure 7: The absolute value of reaction force $R(v, \psi_1)$ at parameters from Section 1.2 – resonance zone.

1.5 Influence of the body mass on the throw coefficient in quasi-steady states

The phenomenon of dynamic elimination, described above, is used in the work of the antiresonance conveyor. The mass of the eliminator is the conveyor trough, while the mass protected is the machine body to which the sources of excitation force are mounted, e.g. electric vibrators. A parameter that is important in the operation of such conveyors is the throw coefficient k_p , which is defined as

$$k_p = \frac{a}{g \cos(\alpha)},\tag{9}$$

or in equation (10)

$$k_p = \frac{Bv^2 \sin(\beta)}{g \cos(\alpha)},\tag{10}$$

where a is the amplitude of normal component of the vibrating trough's acceleration (trough – mass of the eliminator), B is the amplitude of body's and trough's displacements, g is the acceleration of gravity, α is the trough angle to horizontal ($\alpha > 0$ when moving uphill), β is the inclination angle of the steady state trough's trajectory, and ν is the frequency of work.

The throw coefficient, which decides, among other things, on the speed and efficiency of a feed transport, was described by Michalczyk [22]. The limitation of the throw coefficient value causes a reduction in the feed velocity. From the point of view of conveyor's operators, it is important to precisely dose the transported material. When the angular speed ν of the electrovibrators decreases (Figure 15), the transport speed decreases, which is caused by the limited value of the throw coefficient (Figure 8). While passing through the resonance zone, the vibration increases and thus the throw coefficient increases, which

can lead to uncontrolled dosing of additional feed masses. As Figure 8 shows, increasing the body mass with a constant trough mass leads to a reduction of the throw coefficient in the resonance zone, which is an important factor for constructions in the context of precise dosing of the feed mass. The value of the throw coefficient should be above 1 to transport the feed. Below this value ($k_p < 1$), the throw of the feed is impossible. This is the expected value when the feed must be immediately stopped during coasting or when it is not necessary to stop the engine connected with passing through the resonance zone. The increasing throw coefficient can cause uncontrolled dosing of an additional portion of the feed.

Figure 8 shows the quasi-stationary states of operation of the dynamic eliminator for different types of mass m_1 suspensions, which is characterized by various energy absorption coefficients. At an operating frequency of $v = 157 \, \text{rad/s}$, the throw coefficients are identical for both cases, equal to about 3.8. They do not change depending on the mass m_1 and the type of its suspension. Reducing the operating frequency from the state of the antiresonance velocity to enter the resonance zone increases the throw coefficient. As can be seen in Figure 8, lower values of this coefficient characterize the rubber suspension with

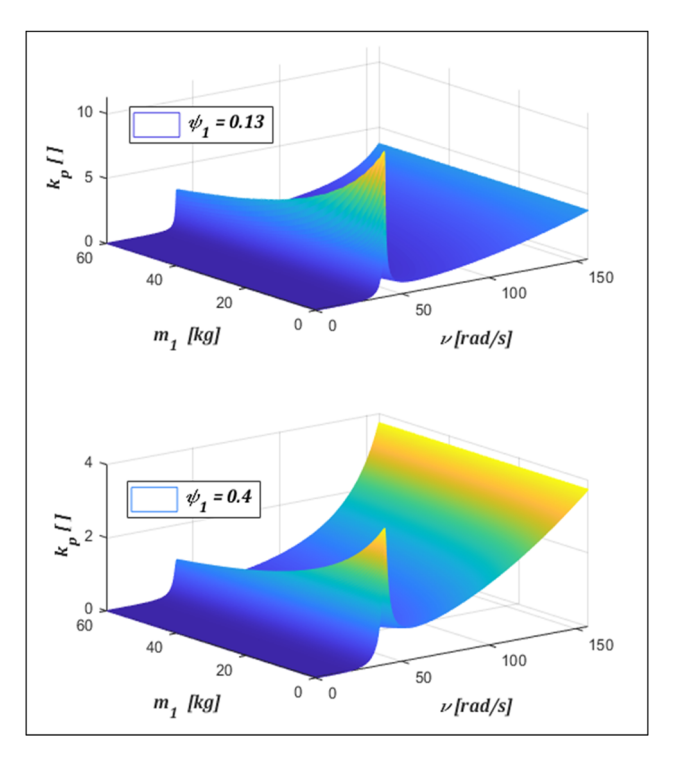


Figure 8: Graphs of the throw coefficient as a function of mass m_1 and exciting frequency (the energy absorption coefficient of the mass m_1 suspension: $\psi_1 = 0.13$ [coil springs] and $\psi_1 = 0.4$ [rubber elements]; $\psi_2 = 0.04$ [leaf springs] for both cases).

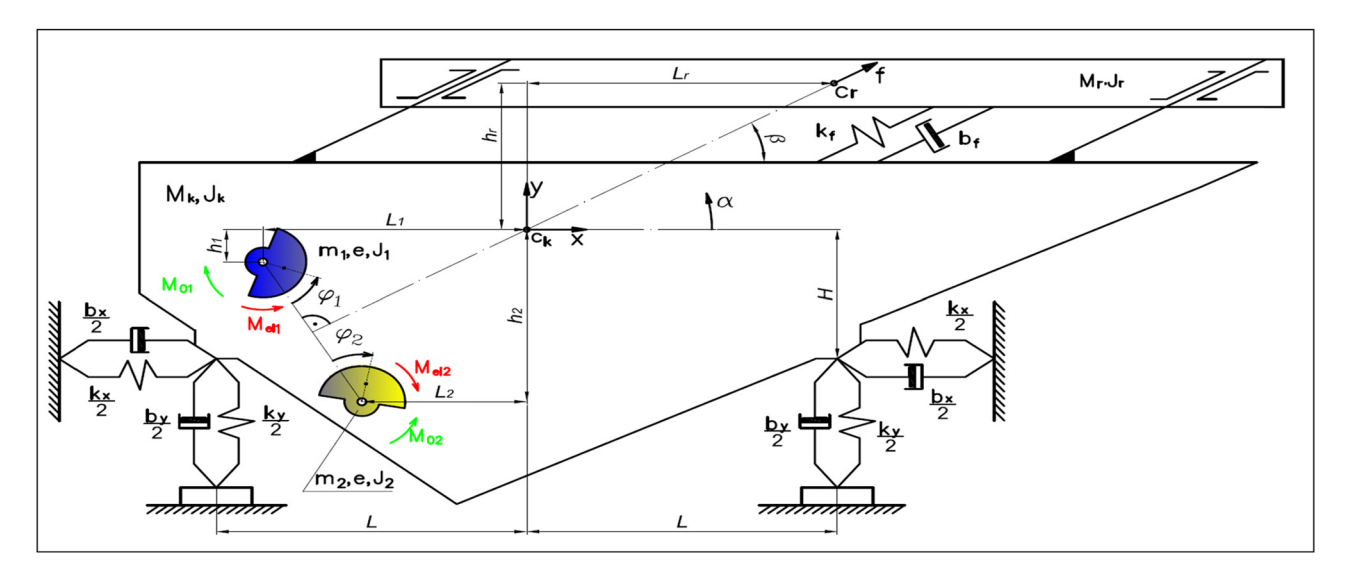


Figure 9: Physical and discrete model of the antiresonance conveyor of six DOFs $(x, y, \alpha, f, \varphi_1, \varphi_2)$.

a higher energy absorption coefficient ($\psi_1 = 0.4$). The use of this type of suspension is therefore the best solution.

2 Dynamic model of the vibratory conveyor with six DOFs

The antiresonance conveyor, as a construction present in the industry, is characterized by the kinematics of a higher number of DOFs. It constitutes the spatial and symmetric system, in which discrete model - the most often - can be reduced to the flat system, which was utilized in creating the physical model (Figure 9). The absolute system, central versus the machine body of axes *OXY* and generalized dislocations x, y, and α (body rotation angle), φ_1 and φ_2 (absolute angles of vibrators rotations), and f (relative dislocation of the trough versus the body), was assumed for a description of the motion of the system in the static equilibrium of the machine without a feed. The model consists of the mass of the body M_k and the mass of the trough M_r and of two inertial vibrators. The trough is assembled to the body by leaf springs. The body is suspended on elements of a dissipative-elastic character attached to the foundation. Counter running vibrators, which are the source of the resulting excitation force acting on the body in the direction of vibrations, were analysed by Michalczyk and Gajowy [15]. The vibrators were arranged in such a way that the bisector, connecting centres of vibrator joints, was passing through the centres of the trough and body masses. Equations concerning the dynamics of the designed conveyor were derived by the method of Lagrange's equations of type II. Solutions to these equations provided, in the further part of this work, several important characteristics.

Physical and geometric parameters of the model (presented in Tables 1 and 2) were selected in such a way that the centres of gravity were overlapping and the trough was inside the body-due to the minimization of the taken cubature. Masses of the body and trough, as well as the stiffness were selected in the same way as for the model of two DOFs with supplementing the additional information on transverse elasticity k_x . The excitation force of the system originates from two inertial vibrators self-synchronizing during operations. During the ideal synchronization, when the difference of phase angles $\varphi_1 - \varphi_2 = 0$, vibrators produce translatory and harmonic force passing exactly through centres of gravity of the trough and body. The self-synchronization effect constitutes the main difference between models of two and six DOFs. This is the most essential problem, which should not be omitted in modelling effects occurring at operations of vibratory conveyors with two independent vibrators.

The real object, from which mass and structure parameters were taken (apart from the body mass, since this was variable during simulations), was made of constructional steel, while suspension elements, i.e. leaf springs joining the trough and body, were made of spring steel. Elastomer springs, Rosta type, were elements of the body suspension on the foundation (described by Cieplok et al. [24]). The total length of the trough of the conveyor, shown in Figure 1, equals 1.5 m.

The set of equations describing the machine motion can be written in a form:

$$\mathbf{M} \cdot \ddot{\mathbf{q}} = \mathbf{Q},\tag{11}$$

where \mathbf{Q} is the matrix of free terms (13), \mathbf{M} is the mass matrix (15), and $\ddot{\mathbf{q}} = \frac{d^2}{dt^2} [x, y, \alpha, f, \phi_1, \phi_2]^T$.

The following boundary conditions were assumed for generalized coordinates:

x(0) = 0,	$\dot{x}(0)=0,$
y(0) = 0,	$\dot{y}(0)=0,$
$\alpha(0)=0$,	$\dot{\alpha}(0)=0,$
$\varphi_1(0)=-\pi/6,$	$\dot{\varphi}_1(0)=0,$
$\varphi_2(0)=-\pi+\pi/6,$	$\dot{\varphi}_2(0)=0,$
f(0)=0,	$\dot{f}(0)=0,$

The static characteristics of Kloss (12) were used to describe the electrical torque of the induction asynchronous motor:

$$M_{el} = \frac{2M_{ut}(\omega_s - \omega_{ut}) \cdot (\omega_s - \omega)}{(\omega_s - \omega_{ut})^2 + (\omega_s - \omega)^2},$$
 (12)

where $\omega = \dot{\phi}_i$, $i = \{1, 2\}$, $\omega_{ut} = 106.6 \text{ rad/s}$, $M_{ut} = 2.046 \text{ Nm}.$

3 Analysis of transient and steady states of numerical simulation of the antiresonance conveyor

3.1 Numerical computing environment

The Matlab environment was applied in solving differential equations describing the discrete nonlinear model of the antiresonance conveyor. In this case, due to a lack of modelling of collisions with transported material. method ode45 with a determined time step was used. The selection of the proper time step was performed by comparing simulation results of the model of the conveyor with the highest frequency of the motor work for various time steps (from 0.01 to 0.00001s). Maximal values of shifts y_{max} are presented in Table 3.

Finally, the time step applied in calculations was 0.0001 s. For this value, solutions are convergent. In comparing simulation results performed with time steps 0.0001 and 0.00001s, the difference between calculated values was equal 1.78×10^{-10} (m), which constitutes such a small

$$\mathbf{Q} = \begin{bmatrix} m_{1} \sin(\beta + \varphi_{1})\dot{\varphi}_{1}^{2}e - m_{2} \sin(\beta - \varphi_{2})\dot{\varphi}_{2}^{2}e - k_{x}(x + H\alpha) - b_{x}(\dot{x} + H\dot{\alpha}) \\ m_{2} \cos(\beta - \varphi_{2})\dot{\varphi}_{2}^{2}e - m_{1} \cos(\beta + \varphi_{1})\dot{\varphi}_{1}^{2}e - k_{y}y - b_{y}\dot{y} \\ L_{1}m_{1} \cos(\beta + \varphi_{1})\dot{\varphi}_{1}^{2}e - h_{2}m_{2} \sin(\beta - \varphi_{2})\dot{\varphi}_{2}^{2}e - L_{2}m_{2} \cos(\beta - \varphi_{2})\dot{\varphi}_{2}^{2}e + \\ + h_{1}m_{1} \sin(\beta + \varphi_{1})\dot{\varphi}_{1}^{2}e - b_{x}(\dot{x} + H\dot{\alpha})H - k_{x}(x + H\alpha)H + \\ -\frac{b_{y}(\dot{y} + L\dot{\alpha})L}{2} + \frac{b_{y}(\dot{y} - L\dot{\alpha})L}{2} - \frac{k_{y}(y + L\alpha)L}{2} + \frac{k_{y}(y - L\alpha)L}{2} \\ - b_{s}\dot{f} - k_{f}f \\ - m_{1}g \sin(\beta + \varphi_{1})e + M_{el1} + M_{01} \\ - m_{2}g \sin(\beta - \varphi_{2})e + M_{el2} + M_{02} \end{bmatrix}.$$

$$(13)$$

On account of the pressure exerted, among others, by the centrifugal force of inertia for the steady motion of vibrators, the resistances to motion moments in rolling bearings are described by approximate dependencies:

$$M_{01} = -m_1 e_1 \dot{\phi}_1^2 \mu d \operatorname{sgn}(\dot{\phi}_1 - \dot{\alpha}) \quad [Nm],$$

$$M_{02} = -m_2 e_2 \dot{\phi}_2^2 \mu d \operatorname{sgn}(\dot{\phi}_2 + \dot{\alpha}) \quad [Nm],$$
(14)

where $\mu = 0.0018$ – coefficient reduced for ball bearings described by Palmgren [25] and d = 0.01 m – shaft spigot diameter of vibrators.

$$M = \begin{bmatrix} m_1 + m_2 + M_k + M_r & 0 & h_1 m_1 + h_2 m_2 - h_r M_r & M_r \cos \beta & m_1 \cos(\beta + \phi_1)e & m_2 \cos(\beta - \phi_2)e \\ 0 & m_1 + m_2 + M_k + M_r & -L_1 m_1 - L_2 m_2 + L_r M_r & M_r \sin \beta & m_1 \sin(\beta + \phi_1)e & m_2 \sin(\beta - \phi_2)e \\ J_k + J_r + L_1^2 m_1 + L_2^2 m_2 + & L_r M_r \sin \beta + -L_1 m_1 \sin(\beta + \phi_1)e + -L_2 m_2 \sin(\beta - \phi_2)e + L_2 m_2 \sin(\beta - \phi_2)e + L_2 m_2 \sin(\beta - \phi_2)e \\ h_1 m_1 + h_2 m_2 - h_r M_r & -L_1 m_1 - L_2 m_2 + L_r M_r & +L_r^2 M_r + h_1^2 m_1 + h_2^2 m_2 & -h_r M_r \cos \beta & +h_1 m_1 \cos(\beta + \phi_1)e & +h_2 m_2 \cos(\beta - \phi_2)e \\ h_1 m_1 \cos(\beta + \phi_1)e & m_1 \sin(\beta + \phi_1)e & -L_1 m_1 \sin(\beta + \phi_1)e & 0 & J_1 + m_1 e^2 & 0 \\ h_1 m_1 \cos(\beta + \phi_1)e & m_1 \sin(\beta + \phi_1)e & -L_1 m_1 \sin(\beta + \phi_1)e & 0 & J_1 + m_1 e^2 & 0 \\ h_1 m_1 \cos(\beta - \phi_2)e & m_2 \sin(\beta - \phi_2)e & -L_2 m_2 \sin(\beta - \phi_2)e & 0 & 0 & J_2 + m_2 e^2 \\ & +h_2 m_2 \cos(\beta - \phi_2)e & 0 & 0 & J_2 + m_2 e^2 \\ \end{bmatrix}.$$

$$(15)$$

Table 1: Geometric parameters

	Symbol of geometric parameter									
Unit	The total length of the gutter	L	н	L ₁	h ₁	L ₂	h ₂	h _r	L _r	β
(m)	1.5	0.5	0.135	0.11	-0.19	-0.11	0.19	0	0	30°

Table 2: Physical parameters

Symbol Value		Unit	Definition	
k_f	k ₂ *	N/m	Stiffness of suspensions	
k_{ν}	k ₁ *	N/m	Stiffness of suspensions	
k_x	$0.5k_{\nu}$	N/m	Stiffness of suspensions	
b_f	b ₂ *	Ns/m	Coefficient of viscous damping	
b_{v}	<i>b</i> ₁ *	Ns/m	Coefficient of viscous damping	
b_x	0.5 <i>b_v</i>	Ns/m	Coefficient of viscous damping	
M_k	10/60	kg	Mass of the body	
M_r	20	kg	Mass of the trough	
$m_{1,2}$	1.49	kg	Unbalanced mass of the vibrator	
J_k	$1/12 \cdot M_k(2.4L)^2$	kg m ²	Central moments of inertia of the body	
J_r	3.75	kg m ²	Central moments of inertia of trough	
$J_{1,2}$	5.96×10^{-4}	kg m ²	Central moments of inertia of unbalanced mass	
e	0.02	m	Radius of a vibrator unbalance	
P	0.12	kW	Asynchronous engine power	
ω_s	157	rad/s	Angular velocity of the synchronous running	

^{*}Parameters from Section 1.2.

difference that results for the time step of 0.0001s were considered the correct ones, from the point of view of the methodology of numerical calculations (Table 4).

3.2 Conveyor not loaded by a feed mass – start-up process of the antiresonance conveyor

Figure 10 shows that the vertical displacement *y* of the centre of gravity of the body mass is very low after a short time. The conveyor operates within the antiresonance range, approximately 157 rad/s, at which the mass of the body stops. This additional field of forces generated

Table 3: Maximal values of shifts y_{max} in the steady state for various time steps

d <i>t</i>	0.01 (s)	0.001 (s)	0.0001 (s)	0.00001 (s)
y _{max} *	1.0396 × 10 ⁻⁵ (m)	$1.0692102 \times 10^{-5} \text{ (m)}$	$1.0693875 \times 10^{-5} \text{ (m)}$	$1.0694053 \times 10^{-5} \text{ (m)}$

^{*}In steady state between 99.91 and 100 s.

by the vibrating trough causes counterbalancing of the force originating from operating electrovibrators, which experience a self-synchronization and generate only a resulting force passing through the body centre of gravity. Figure 10 also shows the relative displacement of the trough versus the body. The trough, in the presented model, serves as the dynamic eliminator, as presented in Figure 2.

The numerical solution of the mathematical model of the vibratory conveyor described by equation (11) indicates that, in the start-up moment, the model passes through resonance frequencies exciting the transient resonance. However, Figure 11 indicates that when the angular frequency of electrovibrators is set at the level of anti-resonance frequency, angular displacements disappear, and the model operates in a very similar way to the model of two DOFs (Figure 2).

3.3 Determination of the optimal mass of the body

In order to determine the optimal mass of the body, the operations of the conveyor at various masses of the body

Table 4: Differences of maximal shifts y_{max} in the steady state for various time steps

Compared time steps dt	0.01 ÷	0.001 ÷	0.0001 ÷
	0.001 (s)	0.0001 (s)	0.00001 (s)
Δy_{max}^*	$2.96\times10^{-7}(\text{m})$	$1.77 \times 10^{-9} \ (m)$	$1.78 \times 10^{-10} (m)$

^{*}Difference in y_{max} in the steady state from 99.91 to 100 s between values for the indicated time steps.

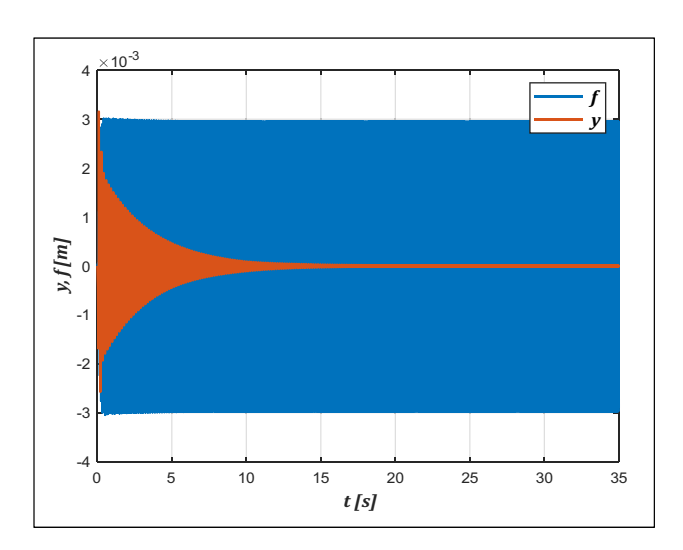


Figure 10: Vertical displacement of the body mass *y* and relative displacement *f* of the trough versus the mass of the body as a time function.

were investigated ($M_k = 10 \div 60$). Simultaneously constant values of the following physical parameters were maintained:

$$M_r = 20 \text{ kg}, \quad m = 2.98 \text{ kg}, \quad e = 0.02 \text{ m},$$

 $k_f = v_{ar}^2 \cdot M_r = 492,800 \text{ N/m}, \quad v_{ar} = 157 \text{ rad/s}.$

The coefficient of elasticity of the body mass suspension M_k is selected from the vibroinsulation condition and equation (16) determines its value in relation to its value for the mass of the body, $M_k = 20 \text{ kg}$.

$$k_y(M_k) = 66,800 \cdot \frac{M_k + M_r}{20 + M_r} [\text{N/m}].$$
 (16)

Such assumption of the coefficient for various masses of the body $M_k = 10 \div 60$ kg assures the same static deflection and the proper vibroinsulation of foundations. Energy absorption coefficients were assumed analogically as for the system of two DOFs:

 ψ_1 = 0.4 – energy absorption coefficient of rubber elements and

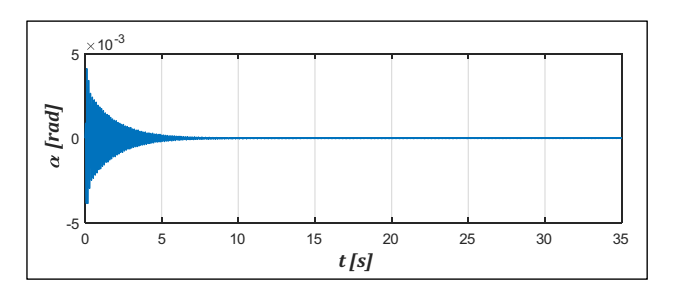


Figure 11: Angular displacement of the body and trough of the conveyor model.

 $\psi_2 = 0.04$ – energy absorption coefficient for elements of the flat metal springs type.

For such assumed data, the diagrams of force $F_w(\omega)$ transmitted to the foundation were obtained as the function dependent on the synchronous frequency of the range $\omega = 0-250\,\mathrm{rad/s}$. The value of the synchronous frequency, which constituted the base for the determination of the moment – given by the asynchronous motor and described by the Kloss formula – was changing according to the dependency described by formula (17) at the simulation time $t = 0-500\,\mathrm{[s]}$.

$$\omega = 157 \cdot \frac{t}{300} [\text{rad/s}]. \tag{17}$$

Such formulation of ω allowed us to achieve the amplitude–frequency characteristics of forces transmitted to the foundation, similar to quasi-stationary conditions.

The force F_w transferred to the ground by the conveyor model with six DOFs was calculated as the resulting value of the sum of the elasticity and damping forces from

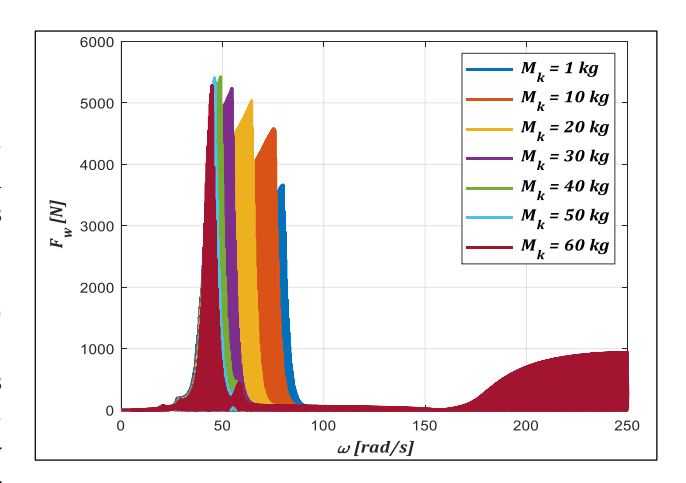


Figure 12: Amplitude–frequency characteristics of the resulting force transmitted to the foundation as a function of the synchronous frequency of asynchronous induction motor for various masses of the body – from 1 kg to 60 kg for the system with six DOFs.

both supports of the conveyor model in the direction of the *OX* and *OY* axes, so it was the total force generated on the ground. The same force was adopted as a comparative criterion for the vibroinsulation of a model with specific parameters. In addition to the resulting force, the moment was also transferred to the ground as a pair of forces, resulting from the angular vibrations of the model.

Figure 12 indicates that forces transmitted to the foundation for all masses are the smallest at the antiresonance frequency $v_{ar} = 157 \text{ rad/s}$. The antiresonance zone is clearly different for each ratio of the trough to the body mass. In a similar manner as for the system of two DOFs, the resulting force transmitted to the foundation is the highest at passing through the transient resonance for the highest masses of the body (from 30 to 60 kg).

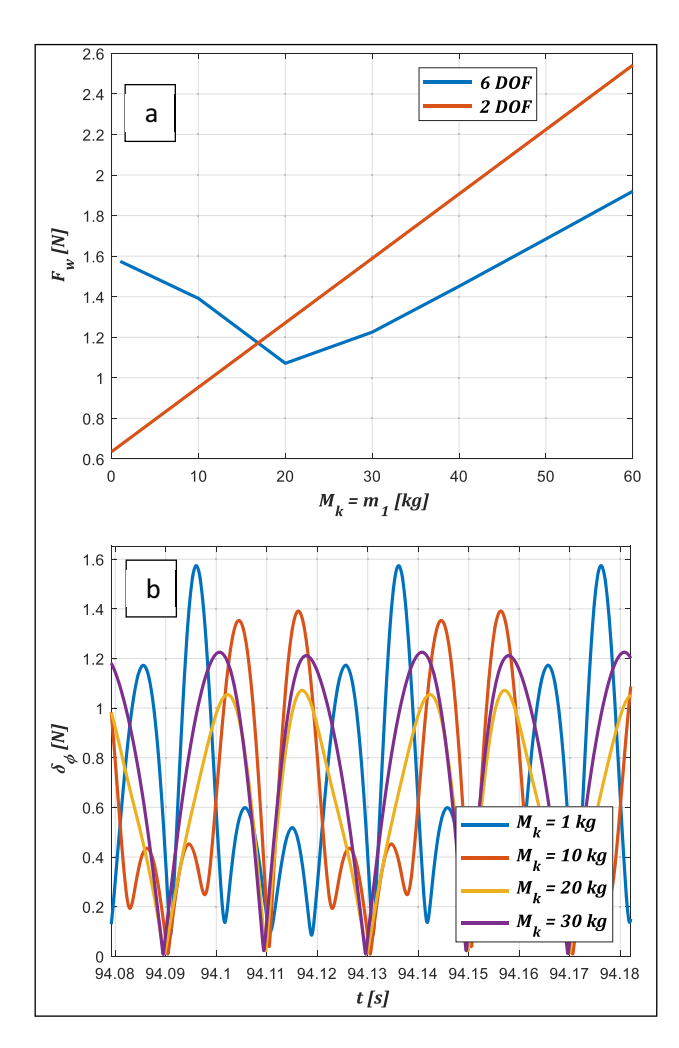


Figure 13: (a) Force transmitted to the foundation at the steady state for systems of two and six DOFs at the antiresonance frequency of 157 rad/s as a function of various masses of the body $M_k = m_1$ at maintaining the mass of the trough $M_r = m_2 = 20$ kg = const, and (b) absolute value of the disphasing angle of vibrators at the body mass of 1, 10, 20, and 30 kg for the system with six DOFs.

The comparison diagram of forces transmitted to the foundation at the steady state, by systems of two and six DOFs, as a function of the body mass is presented in Figure 13a. It can be seen that at the body mass $M_k = m_1$ higher than 20 kg the force transmitted to the foundation increases (at the antiresonance frequency).

Different behaviours of these two models are seen at smaller masses of the body (from 1 to 20 kg), where the force transmitted to the foundation decreases in the system of six DOFs. This can be a result of the self-synchronization effect occurring in this model. The self-synchronization effect was investigated in this work by disphasing angle of vibrators $\delta_{\varphi} = \varphi_1 - \varphi_2$ (Figure 13b). It shows explicitly that at too small masses of the body, the disphasing of vibrators is higher causing disturbances of operations in the antiresonance zone as well as increasing forces are transmitted to the foundation since the excitation force – generated by rotating masses – does not pass exactly by the centre of gravity of the system (investigation of over-resonance conveyors by Michalczyk and Czubak [26]). Value $\delta_{\varphi} = 0$ determines the disphasing angle corresponding to the desired synchronization.

As it results from Figure 14, the resulting force transferred to the ground by a conveyor model with six DOFs – during speeding up of the machine – decreases along with an increase of body mass suppression coefficient. It indicates the need of using elements of the body suspension with significant damping. Therefore, there is a similarity between models with two and six DOFs, as shown in Figure 13a. The differences in the values of resulting forces are consedby the generated angular vibrations of the model with a larger number of generalized coordinates. The energy pumped into the system

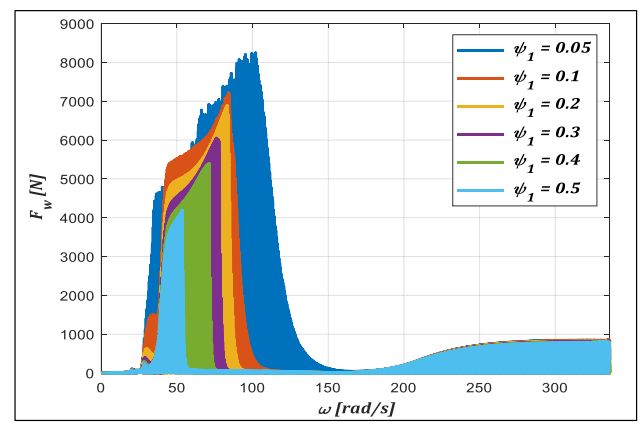


Figure 14: Amplitude–frequency characteristics of forces transmitted to the foundation as the function of the synchronous frequency of asynchronous induction motor, for various values of the energy absorption coefficient of mass suspension M_{k_r} ($M_k = M_r = 20 \text{ kg}$), $\psi_2 = 0.04$ for the system with six DOFs.

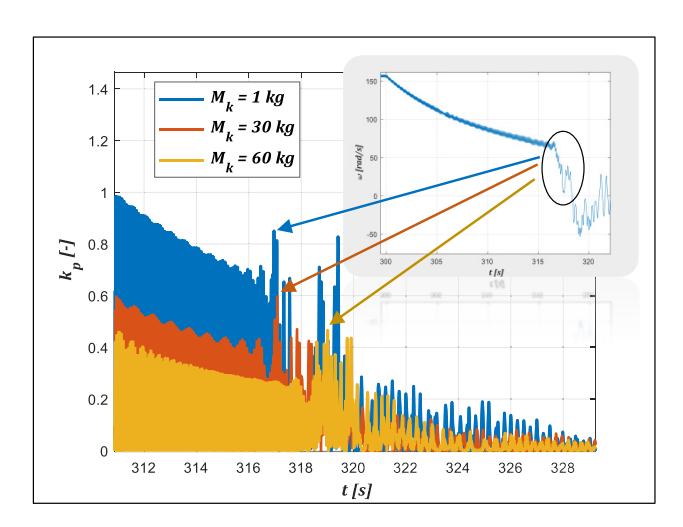


Figure 15: The throw coefficient as a function of time and body mass M_k for both cases $\psi_1 = 0.4$, $\psi_2 = 0.04$ and trough mass $M_r = 20$ kg (motors off at the 300th second – loss of angular velocity and enter to the resonant zone [around the 316th second]).

is stored in angular vibrations, which reduces the total forces transferred to the ground. It should be noted that the appearance of angular vibrations transfers the moment of force to the ground, which is also a negative phenomenon.

The coefficient of throw for the model with six DOFs during coasting (engines off in 300 s) shows similar relations, at different body masses (Figure 15), to the quasistationary states shown in Figure 8 for a system with two DOFs (run-up). The use of a heavier body leads to a reduction of the throw coefficient and thus to the vibration amplitudes of the body and the trough. This prevents uncontrolled dosing of material, with the need to stop quickly transporting the feed. Figure 15 shows the loss of the angular velocity of one of the electric vibrators. A characteristic point is an area near the 316th second in which the system enters the resonance zone and there is a rapid release of energy to the body and trough. In this area, the throw coefficients assume values less than 1 ensuring the stopping of the feed transportation. The smaller the value of the throw coefficients, the better the results of stopping transport.

4 Conclusions

Based on the presented research results, the following conclusions can be drawn:

(1) Forces transmitted to the foundation do not depend, in the analysed conveyors, on the damping coefficient of elements supporting the body on the foundation.

- (2) Forces transmitted to the foundation are significantly dependent on the damping of the trough suspension on the body. The lower the damping coefficient, the smaller the forces transmitted to the foundation.
- (3) The weight of the body should be similar to the weight of the gutter since its selection essentially influences the values of forces transmitted to the foundation. Theoretically, this mass can be as small as possible; however, in a system in which the self-synchronization of motors occurs, a very small body mass can disturb this synchronization, causing an increase of forces transmitted to foundations (Figure 13a).
- (4) At slow passing through the resonance zone at the machine start-up, conveyors of the heaviest frames generate the highest forces transmitted to the foundation. It results from the need to obtain self-synchronization of vibrators in a quasi-stable state at passing the resonance zone.
- (5) The greater weight of the conveyor body reduces the throw coefficient during the coasting and thus enables the precise dosing of the feed. This results from the fact that the total kinetic energy of the system, related to movements of the trough and vibrators, is during coasting transferred into vibrations of the frame, in which the larger mass decreases its amplitude.

Acknowledgments: The work is included in the framework of the Department of Mechanics and Vibroacoustics. 16.16.130.942.

Conflict of interest: Authors state no conflict of interest.

References

- Fischer H. Zur Kenntnis der Fordervorrichtungen fur Sammelkorper. Z des Ver Dautacher Ing. 1891;33.
- [2] Frahm H. Device for damping vibrations of bodies. US Patent No. 989958; 1909.
- [3] Jiao C, Liu J, Wang Q. Dynamic analysis of nonlinear antiresonance vibration machine based on general finite element method. Adv Mater Res. 2012;443–444:694–9.
- [4] Liu J, Sun GF. Theory of anti-resonant vibrating machine with application. J Northeastern Univ (Nat Sci). 1995;16(1):82–6.
- [5] Liu J, Sun G, Tang B, Wen B. Application of antiresonant theory in vibration utilization engineering. Proc Ninth World Congr Theory Mach Mechanism. 1995;8:1093-7.
- [6] Long G, Tsuchiya T. Vibratory conveyors. US Patent No. 2,951,581; 1960.
- 7] Carmichael D. Excited Frame Vibratory Conveying Apparatus for Moving Particle Material. US Patent 4 313 535; 1982.

- Liu J, Li Y, Liu J, Xu H. Dynamical analysis and control of driving point anti-resonant vibrating machine based on amplitude stability. Chin J Mech Eng. 2006;1:1.
- Zhao B, Gao H. Amplitude Control for a driving point antiresonant vibrating screen based on fuzzy self-tuning ID control. J Liaoning Provincial Coll Commun. 2009;1:34-7.
- [10] Ribic A. High-performance feedback control of electromagnetic. Vibratory Feeder Ind Electron. 2010;57(9):3087-94.
- [11] Despotovic Z, Stojiljkovic Z. Power converter control circuits for two-mass vibratory conveying system with electromagnetic drive: simulations and experimental results. IEEE Trans Ind Electron. 2007;54(1):453-66.
- [12] Czubak P. Reduction of forces transmitted to the foundation by the conveyor or feeder operating on the basis of the Frahm's eliminator, at a significant loading with feed. Arch Min Sci. 2020;57(4):1121-36.
- [13] Klemiato M, Czubak P. Event driven control of vibratory conveyors operating on the Frahm's eliminator. Arch Metall Mater. Polish Academy of Sciences. Committee of Metallurgy. Institute of Metallurgy and Materials Science. 2015:60(1):19-25.
- [14] Czubak P. Vibratory conveyor of the controlled transport velocity with the possibility of the reversal operations. J Vibroengineering. 2016;18(6):3539-47.
- [15] Michalczyk J, Gajowy M. Operational properties of vibratory conveyors of the antiresonance type. Arch Min Sci. 2018;63(2):301-19.
- [16] Hou Y, Peng H, Fang P, Zou M, Liang L, Che H. Synchronous characteristics of two excited motors in an antiresonance

- system. J Adv Mech Design Syst Manuf. 2019;13(3):JAMDSM0050.
- [17] Li X, Shen T. Dynamic performance analysis of nonlinear antiresonance vibrating machine with the fluctuation of material mass. J Vib Eng. 2012;18(2):978-88.
- [18] Sturm M. Two-mass linear vibratory conveyor with reduced vibration transmission to the ground. Vibroeng Proce. 2017:13:20-3.
- [19] Sturm M, Pešík L. Two-mass linear vibratory conveyor. 58th ICMD 6-8. Prague: Czech Republic; September 2017.
- [20] Thomson W. Theory of vibrations with applications. New York: Pearson; 1997.
- [21] Den Hartog JP. Mechanical vibrations. New York: McGraw-Hill Book Company, INC; 1956.
- [22] Michalczyk J. Maszyny wibracyjne, obliczenia dynamiczne, drgania, hałas. Vibratory machines, dynamic calculations, vibrations, noise. Warsaw: WNT; 1995.
- [23] Michalczyk J, Cieplok G. Wysokoefektywne układy wibroizolacji i redukcji drgań. Highest effective vibroinsolaition and vibration reduction systems. Kraków: Collegium Columbinum; 1999.
- [24] Cieplok G, Wójcik K, Michalczyk K, Sikora W. Equivalent parameters of metal-elastomer vibroinsulators. Vib Phys Syst. 2020;31(2):2020204.
- [25] Palmgren A. Rolling bearings. Warsaw: PWT; 1951.
- [26] Michalczyk J, Czubak P. Influence of collisions with a material feed on cophasal mutual synchronisation of driving vibrators of vibratory machines. J Theor Appl Mech. 2010;48(1):155-72.